Supplementary information

Supplementary materials and methods

Strains

The following strains were used in this work: *epg-6(bp242)*, *atg-2(bp576)*, *atg-3(bp412)*, *epg-1(bp414)*, *epg-8(bp251)*, *epg-5(tm3425)*, *sqst-1(ok2892)*, *epg-7(tm2508)*, *let-7(n2853)*, *atg-7(bp422)*, *lsy-6(ot71)*, *lsy-6(ot150)*, *alg-1(gk214)*, *ain-1(bp299)*, *ain-1(ku322)*, *dcr-1(bp132)*, *sea-2(bp283)*, *lin-41(ma104)*, *let-60(n1046)*, *bpIs151(sqst-1::gfp*, *unc-76)*, *bpIs255(alg-2::gfp*, *rol-6)*, *bpIs68(ain-1::gfp*, *rol-6)*, *zaIs5(gfp::alg-1*, *rol-6)*, *pkIs2256 (alg-2::HA, rol-6)*, *ctIs39(hbl-1::gfp*, *rol-6)*, *otIs114(lim-6^{pro}::gfp*, *rol-6)*, *bpIs33(col-10::gfp::lin-41(3'UTR))*, *wIs51(scm::gfp)* and *gaIs37(EF1α-D-mek(gf) + hs-mpk-1(wt))*. All experiments are performed at 20 ^{o}C unless otherwise noted.

Reporter construction

Reporters for *ain-1, ain-2* and *alg-2* had *gfp* inserted at the C-terminus. The *alg-2::gfp* and *ain-2::gfp* reporters were constructed by a PCR-fusion based approach. The fused PCR products were derived from two overlapping PCR fragments. One fragment contained about 2 kb of promoter and the entire genomic coding region of *alg-2* (fosmid WRM0629aG12 25,004-32,332) and *ain-2* (B0041, nt10,155–16,177). The other fragment contained *gfp* and the *unc-54* 3'UTR of pPD95.79. *ain-1::gfp* was a gift from the Min Han lab. The fusion PCR product or clone was co-injected with pRF4 (*rol-6*) into wild-type animals.

RNAi experiments

Single-stranded RNA was transcribed from T7- and SP6-flanked PCR templates for RNAi. ssRNAs were annealed and injected into animals. The DNA templates used for RNA synthesis were: *lgg-1* (C32D5, nt35232-35666), *epg-2* (cDNA, nt336-1075).

Antibody preparation

A fragment of AIN-1 (amino acids 343-490) was cloned into pET-21b, expressed as a His-tagged fusion protein in *E. coli* BL21. Polyclonal antibodies against purified proteins were raised in rats.

Quantitative real-time RT-PCR

Total RNAs were extracted using Trizol reagent (Invitrogen, 15596-026) according to the manufacturer's protocol. Quantitative PCR reactions were performed using a SYBR RT-PCR kit (TaKaRa) and a Mastercycler-ep realplex machine (Eppendorf). *actin* was used as an internal control. Error bars indicate the standard deviation (SD) of four independent experiments.

Stress assay

Embryos were placed on 3% agarose pad with a drop of M9 buffer and then covered with a coverslip. GFP::ALG-1 and ALG-2::GFP in autophagy mutants were diffusely localized in the cytoplasm when the slides were viewed immediately, while they gradually accumulated into aggregates when the slides were viewed 10 minutes later.

In vivo Co-IP assay

Extracts of wild type or animals carrying an *alg-2::HA* transgene were prepared and pre-cleaned with 30 μl protein G Sepharose beads for 1 hour at 4 ^{o}C. Extracts

were then immunoprecipitated with anti-LGG-1, anti-HA monoclonal antibody (Sigma), anti-ALG-1(Thermo), or control IgG (anti-GFP monoclonal antibody or anti-HA polyclonal antibody) for 8 h at 4 ^{o}C. 50 µl protein G Sepharose beads were added and incubated overnight. After five washes, the immunoprecipitates were analyzed by Western blotting using the corresponding antibody.

***In vitro* pull-down assay**

cDNAs encoding AIN-1 and fragments of AIN-1 were cloned into pET-21b(+) (for His fusion) or pMAL-C2X (for MBP tagging). cDNAs encoding LGG-1 was cloned into pET-21b(+) (for His fusion) or pGEX-6P-1 (for GST fusion). GST-fusion proteins or MBP-fusion proteins were incubated with His-tagged proteins and glutathione Sepharose beads (for GST fusion proteins) or Amylose resin (for MBP fusion proteins). Bound proteins were analyzed by western blot using an anti-His antibody.

Supplementary figure legends

Fig S1| Elevated expression of reporters for *hbl-1* and *lin-41* in *let-7* mutants is not affected by simultaneous loss of autophagy activity

(A-C) Confocal images showing expression of *hbl-1::gfp::hbl-1* reporter in ventral nerve cord in wild type (A), *let-7* (B) and *epg-6; let-7* (C) at the young adult stage. Images were taken using the same exposure time.

(D) Distribution of relative fluorescence intensity of *hbl-1::gfp::hbl-1* in 50 unit areas in ventral nerve cord in the indicated strains.

(E-G) Confocal images showing expression of *col-10::gfp::lin-41(3'UTR)* reporter in hypodermal cells in wild type (E), *let-7* (F) and *lgg-1(RNAi); let-7* (G) at the young adult stage.

(H) Distribution of relative fluorescence intensity of *col-10::gfp::lin-41(3'UTR)* in 50 unit areas of hypodermal cells in the indicated strains. Black lines in (D,H) represent the average fluorescence intensity of the reporter in each strain. *p* values are determined by student's two tailed unpaired *t*-test in (D,H).

Scale bars in (A-C) and (E-G): 10 μm.

Fig S2| Autophagy mutants show accumulation of AIN-1::GFP, ALG-2::GFP and GFP::ALG-1 puncta

(A-B) AIN-1::GFP accumulates into numerous aggregates in the embryos of *atg-2* (A) and *atg-3* (B) mutants. Scale bar: 10 μm for whole embryo. *C. elegans* embryos remain the same size during embryogenesis and loss of autophagy activity has no effect on the embryo size. Thus, scale bars for embryos are only shown once in each figure.

(C) Endogenous AIN-1 protein levels are elevated in *atg-2, epg-8* and *epg-6* mutants compared with wild type animals at the adult stage.

(D) Real-time RT-PCR analysis indicates that levels of *ain-1* mRNA remain unchanged in autophagy mutants compared with wild-type animals. Error bars indicate the standard deviation of four experiments. wt: wild type.

(E-F) AIN-2::GFP diffusely localizes in the cytoplasm during embryonic stages in

wild type animals (E) and its expression pattern is not changed in autophagy mutants (F).

(G) ALG-2::GFP aggregates dramatically increase in *atg-3* mutant embryos under stress conditions.

(H) Number of GFP::ALG-1 aggregates per focal plane in the indicated strains. Four embryos were examined.

(I-J) GFP::ALG-1 diffusely localizes in the cytoplasm during embryonic stages in wild type. (I): Nomarski image of the embryo shown in (J).

(K) GFP::ALG-1 does not form aggregates in *epg-6* mutant embryos under normal conditions.

(L) GFP::ALG-1 accumulates into a large number of aggregates in *epg-6* mutant embryos under stress condition.

(M) Western blot analysis shows that levels of endogenous ALG-1 protein are elevated in *atg-2, epg-8* and *epg-6* mutants compared with wild type at embryonic stage.

(N-O) Real-time RT-PCR analysis of *alg-2* (N) and *alg-1* (O) mRNA levels in wild type and autophagy mutants. Error bars show the standard deviation of four experiments.

(P) AIN-1::GFP accumulated into aggregates in *lgg-1(RNAi); sqst-1* mutants.

Fig S3| ALG-2::GFP and GFP::ALG-1 aggregates colocalize with SQST-1 aggregates in autophagy mutants

(A-D) ALG-2::GFP and endogenous SQST-1 are weakly expressed and diffusely localized in wild-type embryos.

(E-H) ALG-2::GFP aggregates colocalize with SQST-1 aggregates in *atg-3* mutant embryos. Scale bar: 10 μm for insets that show a magnified view.

(I-L) ALG-2::GFP aggregates are separable from PGL granules, detected by anti-SEPA-1, in *atg-3* mutant embryos.

(M-P) Colocalization of ALG-2::GFP aggregates with LGG-1 puncta in *epg-6* mutant embryos.

(Q-T) GFP::ALG-1 aggregates colocalize with SQST-1 aggregates in *atg-3* mutant embryos.

(U-X) GFP::ALG-1 aggregates are separable from PGL granules in *atg-3* mutant embryos.

(Y) % of ALG-2::GFP aggregates colocalized with SQST-1 aggregates, SEPA-1 aggregates and LGG-1 puncta in autophagy mutants. Error bars indicate the standard deviation (SD) of four examined embryos.

(Z) % of GFP::ALG-1 aggregates colocalized with SQST-1 aggregates and SEPA-1 aggregates in *atg-3* mutants. Error bars indicate the standard deviation (SD) of four examined embryos.

(A2) No ALG-2::GFP aggregates are formed in *sqst-1* mutant embryos even under stress conditions.

(B2) ALG-2::GFP aggregates accumulate in *epg-7* mutant embryos under stress conditions.

Fig S4| ALG-1 and ALG-2 do not interact with LGG-1 and AIN-1 interacts with LGG-1 independent of the LIR motif

(A-B) Co-immunoprecipitation assays showing no interaction between ALG-1 and LGG-1. Extracts from wild type animals were precipitated with anti-LGG-1 antibody (A), anti-ALG-1 antibody (B), or control IgG (anti-HA antibody), then analyzed by Western blot with anti-ALG-1, anti-LGG-1 antibody and anti-Actin.

(C) ALG-2 fails to interact with LGG-1 in a co-immunoprecipitation assay. Extracts from animals expressing ALG-2::HA were precipitated with anti-HA antibody or control IgG (anti-GFP antibody), then analyzed by Western blot with anti-HA, anti-LGG-1 or anti-Actin antibody.

(D-F) AIN-1 directly binds to LGG-1 in *in vitro* pull-down assays. GST-tagged LGG-1 immobilized on glutathione Sepharose beads was incubated with His-tagged full-length (D) and truncated (E-F) AIN-1 proteins. The retained proteins were analyzed by SDS-PAGE with anti-His-antibody. Ten percent of the His fusion proteins used for pull-down are shown as input. Corresponding Ponceau-stained blots show the amount of proteins used for pull-down.

(G-I) Mutating either one (G-H) or two LIR motifs (I) in AIN-1 does not alter LGG-1 binding. Mutant 1: AIN-1(343-490) with ^{437}WGEL^{440} mutated to ^{437}AGEA^{440}. Mutant 2: AIN-1(343-490) with ^{462}WNDL^{465} mutated to ^{462}ANDA^{465}. Mutant 1+2: AIN-1(343-490) with ^{437}AGEA^{440} and ^{462}ANDA^{465}.

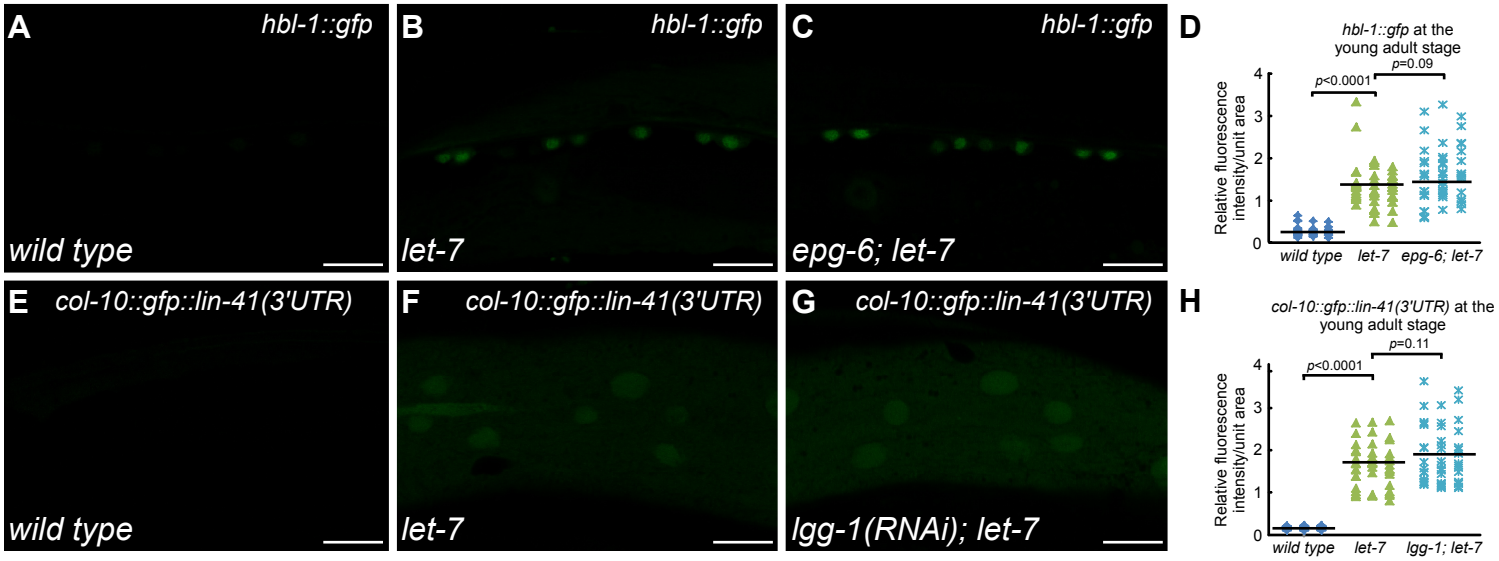
A
hbl-1::gfp
wild type
B
hbl-1::gfp
let-7
C
hbl-1::gfp
epg-6; let-7
D
hbl-1::gfp at the young adult stage
p=0.09
p<0.0001
Relative fluorescence intensity/unit area
0
1
2
3
4
wild type
let-7
epg-6; let-7
E
col-10::gfp::lin-41(3'UTR)
wild type
F
col-10::gfp::lin-41(3'UTR)
let-7
G
col-10::gfp::lin-41(3'UTR)
lgg-1(RNAi); let-7
H
col-10::gfp::lin-41(3'UTR) at the young adult stage
p=0.11
p<0.0001
Relative fluorescence intensity/unit area
0
1
2
3
4
wild type
let-7
lgg-1; let-7

Figure S1

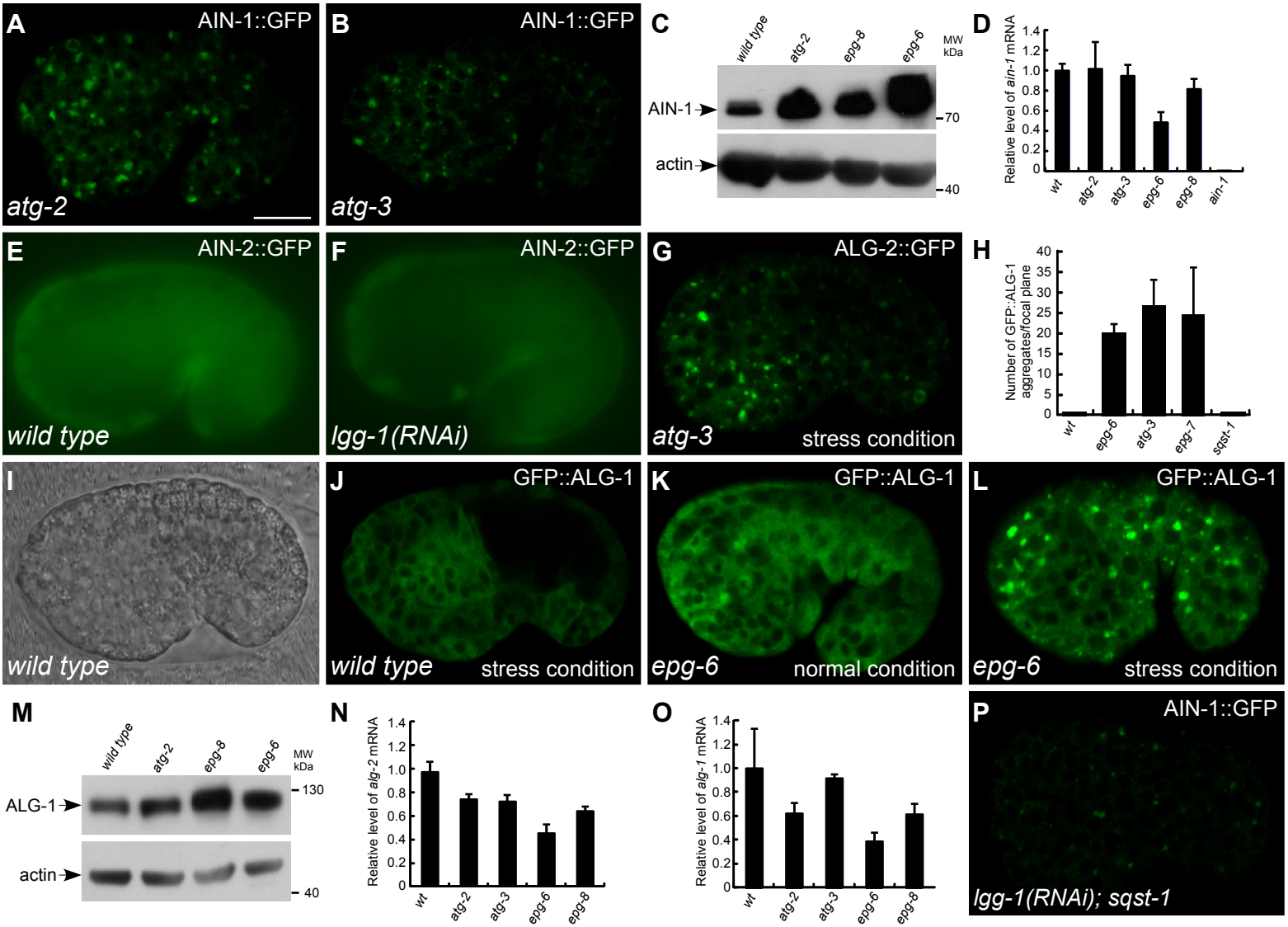
A
AIN-1::GFP
atg-2
B
AIN-1::GFP
atg-3
C
wild type
atg-2
epg-8
epg-6
MW kDa
AIN-1
70
actin
40
D
Relative level of ain-1 mRNA
wt
atg-2
atg-3
epg-6
epg-8
ain-1
E
AIN-2::GFP
wild type
F
AIN-2::GFP
lgg-1(RNAi)
G
ALG-2::GFP
atg-3
stress condition
H
Number of GFP::ALG-1 aggregates/focal plane
wt
epg-6
atg-3
epg-7
sqst-1
I
wild type
J
GFP::ALG-1
wild type
stress condition
K
GFP::ALG-1
epg-6
normal condition
L
GFP::ALG-1
epg-6
stress condition
M
wild type
atg-2
epg-8
epg-6
MW kDa
ALG-1
130
actin
40
N
Relative level of alg-2 mRNA
wt
atg-2
atg-3
epg-6
epg-8
O
Relative level of alg-1 mRNA
wt
atg-2
atg-3
epg-6
epg-8
P
AIN-1::GFP
lgg-1(RNAi); sqst-1

Figure S2

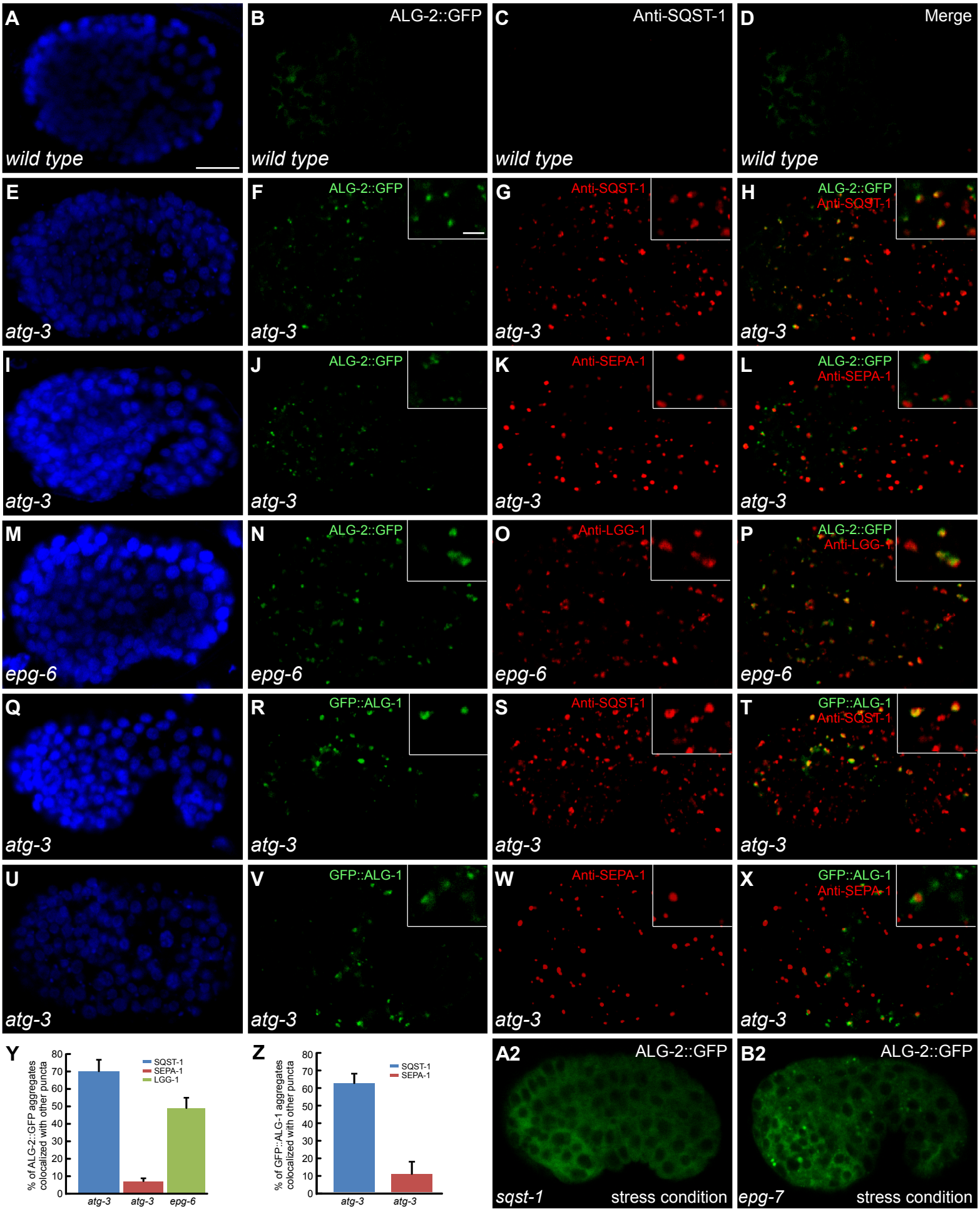
A
wild type
B
ALG-2::GFP
wild type
C
Anti-SQST-1
wild type
D
Merge
wild type
E
atg-3
F
ALG-2::GFP
atg-3
G
Anti-SQST-1
atg-3
H
ALG-2::GFP
Anti-SQST-1
atg-3
I
atg-3
J
ALG-2::GFP
atg-3
K
Anti-SEPA-1
atg-3
L
ALG-2::GFP
Anti-SEPA-1
atg-3
M
epg-6
N
ALG-2::GFP
epg-6
O
Anti-LGG-1
epg-6
P
ALG-2::GFP
Anti-LGG-1
epg-6
Q
atg-3
R
GFP::ALG-1
atg-3
S
Anti-SQST-1
atg-3
T
GFP::ALG-1
Anti-SQST-1
atg-3
U
atg-3
V
GFP::ALG-1
atg-3
W
Anti-SEPA-1
atg-3
X
GFP::ALG-1
Anti-SEPA-1
atg-3
Y
% of ALG-2::GFP aggregates colocalized with other puncta
SQST-1
SEPA-1
LGG-1
atg-3
atg-3
epg-6
Z
% of GFP::ALG-1 aggregates colocalized with other puncta
SQST-1
SEPA-1
atg-3
atg-3
A2
ALG-2::GFP
sqst-1
stress condition
B2
ALG-2::GFP
epg-7
stress condition

Figure S3

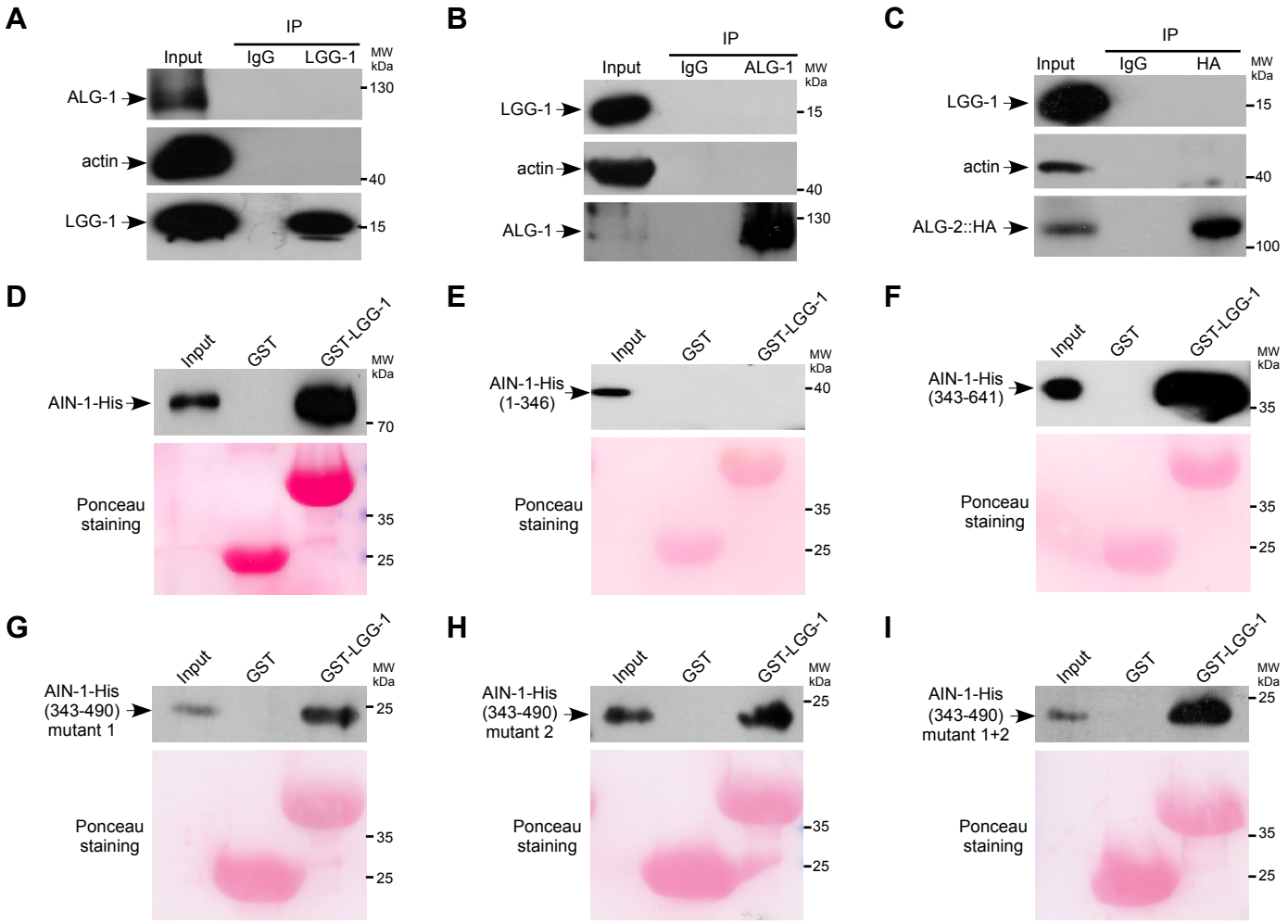
A
IP
Input
IgG
LGG-1
MW kDa
ALG-1
130
actin
40
LGG-1
15
B
IP
Input
IgG
ALG-1
MW kDa
LGG-1
15
actin
40
ALG-1
130
C
IP
Input
IgG
HA
MW kDa
LGG-1
15
actin
40
ALG-2::HA
100
D
Input
GST
GST-LGG-1
MW kDa
AIN-1-His
70
Ponceau staining
35
25
E
Input
GST
GST-LGG-1
MW kDa
AIN-1-His (1-346)
40
Ponceau staining
35
25
F
Input
GST
GST-LGG-1
MW kDa
AIN-1-His (343-641)
35
Ponceau staining
35
25
G
Input
GST
GST-LGG-1
MW kDa
AIN-1-His (343-490) mutant 1
25
Ponceau staining
35
25
H
Input
GST
GST-LGG-1
MW kDa
AIN-1-His (343-490) mutant 2
25
Ponceau staining
35
25
I
Input
GST
GST-LGG-1
MW kDa
AIN-1-His (343-490) mutant 1+2
25
Ponceau staining
35
25

Figure S4